

Supplementary material

Table 4(c). Anisotropic displacement factors (\AA^2)

Atom	U_{11}	U_{22}	U_{33}	U_{12}	U_{13}	U_{23}
Ca1 ^o	0.00936(4)	0.00981(4)	0.00691(4)	0.0	0.0	0.00090(4)
Al1 ^o	0.00633(4)	U_{11}	U_{11}	-0.000145(19)	U_{12}	U_{12}
Al2 ^o	0.00774(5)	0.00488(5)	U_{11}	0.0	0.0	0.0
O1 ^o	0.01081(8)	0.01258(9)	0.01128(7)	-0.00569(8)	0.00251(7)	-0.00328(6)
O2 ^o	0.01011(8)	U_{11}	U_{11}	-0.00174(6)	U_{12}	U_{12}
Ca1b ^o	0.0176(4)	0.0113(3)	0.0094(2)	0.0	0.0	0.0000(2)

Deposited figures

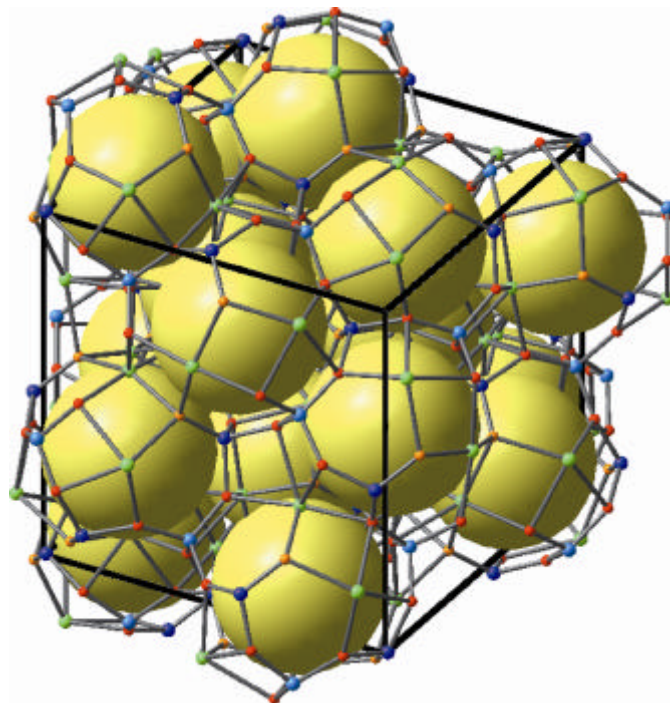


Figure 9 Crystal structure of C12A7 (OK)

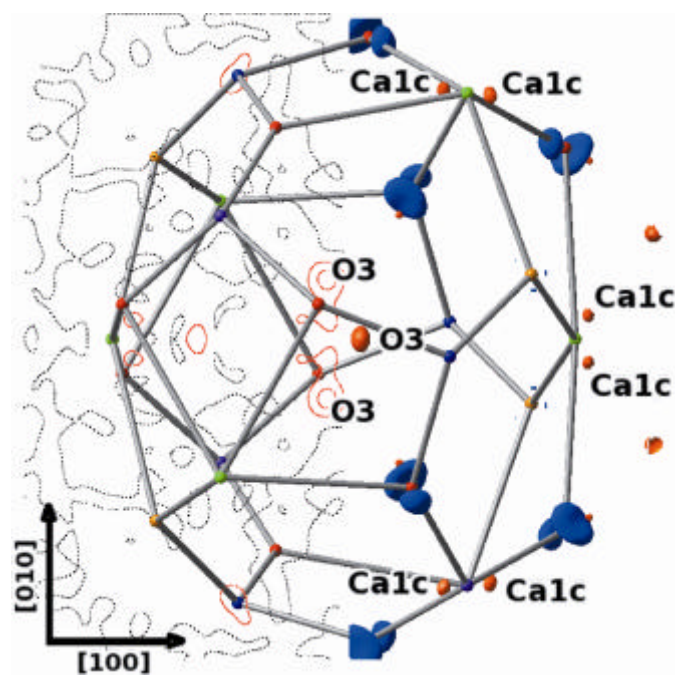


Figure 10 Difference density after Refinement C. Contours at $0.5 \text{ e}\text{\AA}^{-3}$. Equi-density surface at $\pm 1.0 \text{ e}\text{\AA}^{-3}$.

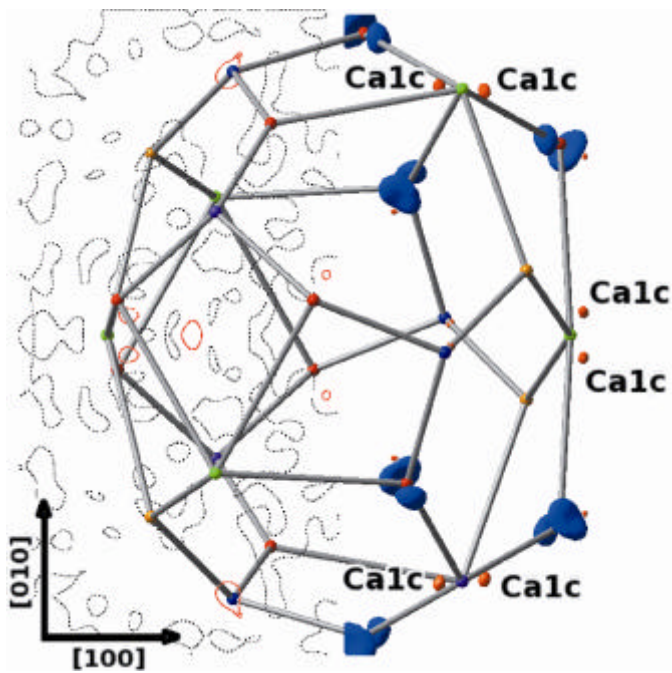


Figure 11 Difference density after Refinement D. Contours at $0.5 \text{ e}\text{\AA}^{-3}$. Equi-density surface at $\pm 1.0 \text{ e}\text{\AA}^{-3}$.

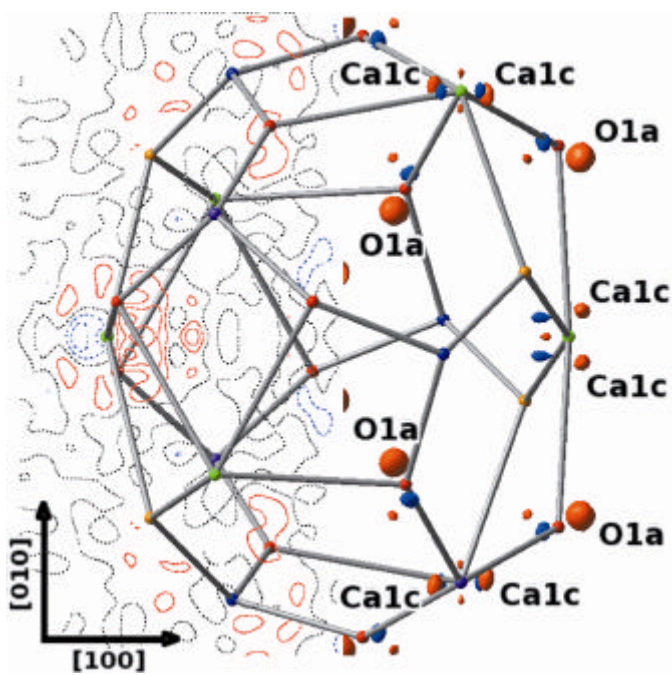


Figure 12 Difference density after Refinement E. Contours at $0.2 \text{ e}\text{\AA}^{-3}$ and equi-density surface at $\pm 0.55 \text{ e}\text{\AA}^{-3}$.

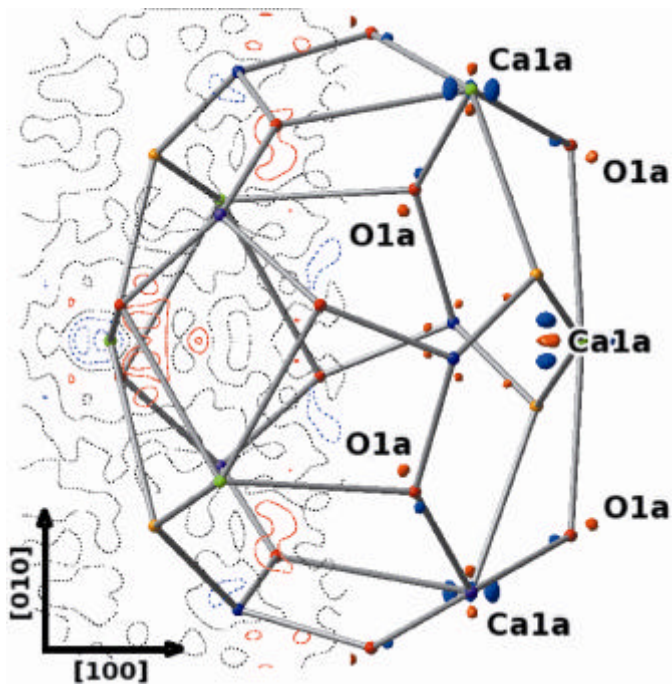


Figure 13 Difference density after Refinement G. Contours at 0.2 eÅ⁻³ and equi-density surface at ±0.45 eÅ⁻³.

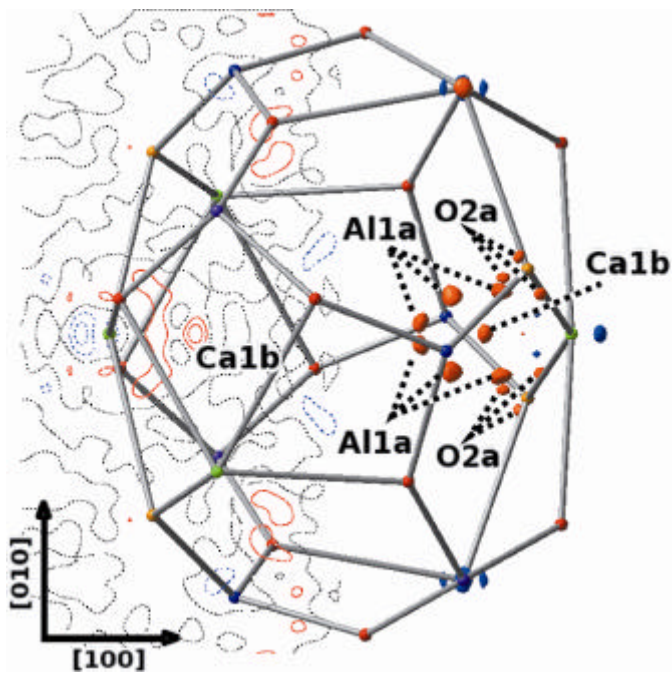


Figure 14 Difference density after Refinement H. Contours at 0.2 eÅ⁻³ and equi-density surface at ±0.37 eÅ⁻³.

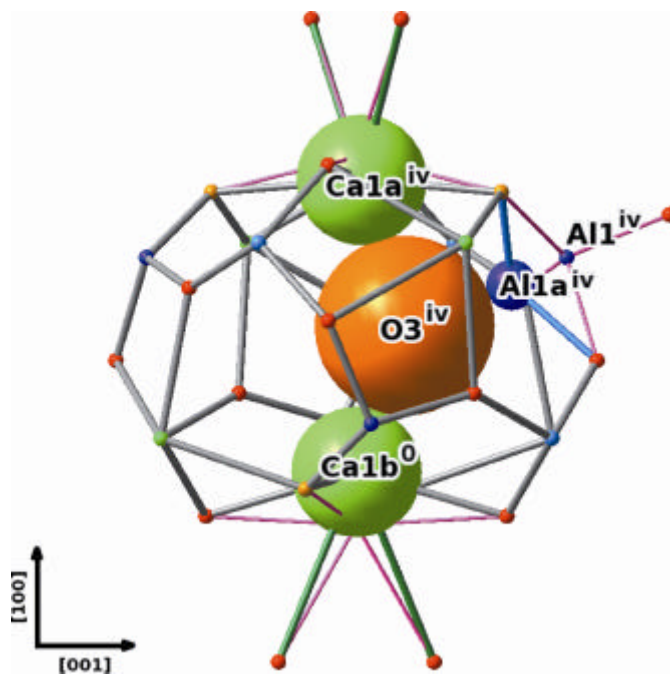


Figure 15 Possible arrangement of the displaced Ca1 ions in the occupied cage. Ca1 ions and O3 aligned as Ca1a^{iv}-O3^{iv}-Ca1b⁰. Radii of the spheres are proportional to the ionic radii.

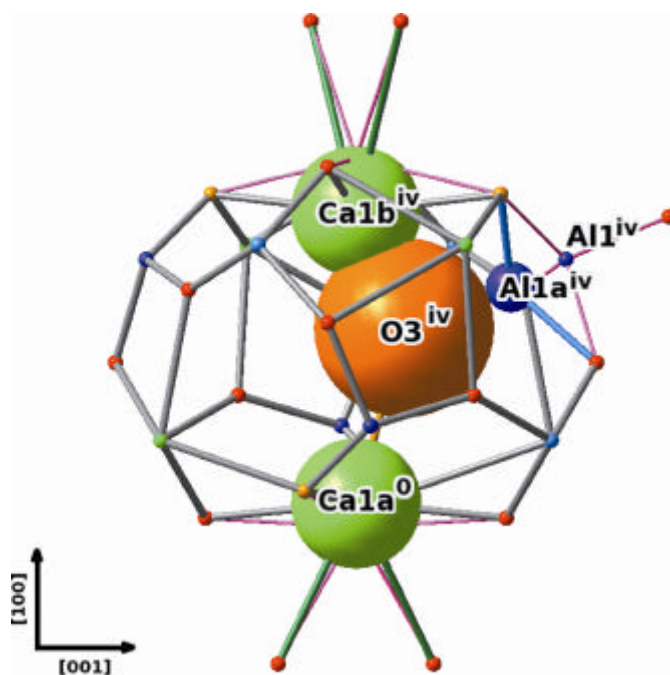


Figure 16 Possible arrangements of Ca1 ions in the occupied cage. Ca1 ions and O3 aligned as Ca1b^{iv}-O3^{iv}-Ca1a⁰. Radii of the spheres are proportional to the ionic radii.

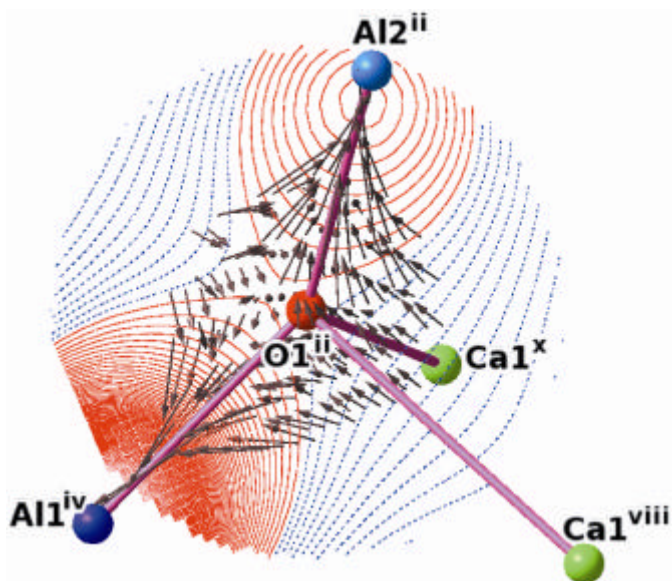


Figure 17 Potential on the plane of Al1^{iv} , O1^{ii} and O1b^{ii} around O1^{ii} in the vacant cage. The potential at O1^{ii} is subtracted from each point in the figure, and contours are as in Fig.5.

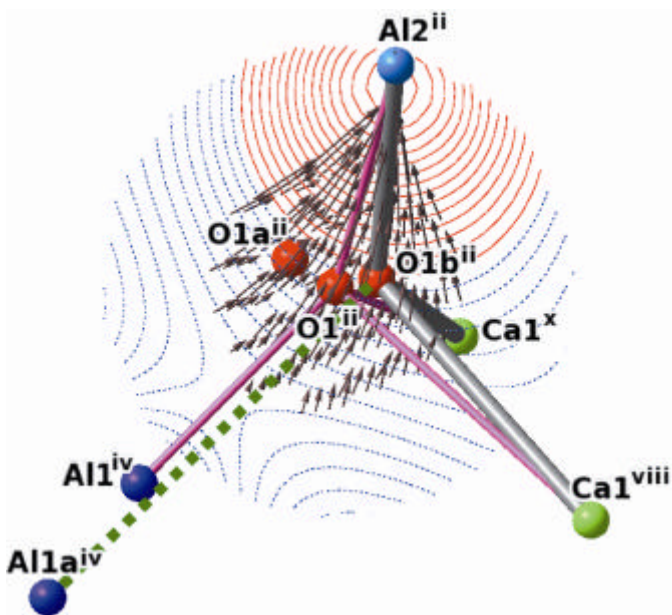


Figure 18 Potential on the plane of Al1^{iv} , O1^{ii} and O1b^{ii} around O1b^{ii} in the occupied cage. The potential at O1^{ii} is subtracted from each point in the figure, and contours are as in Fig.5.

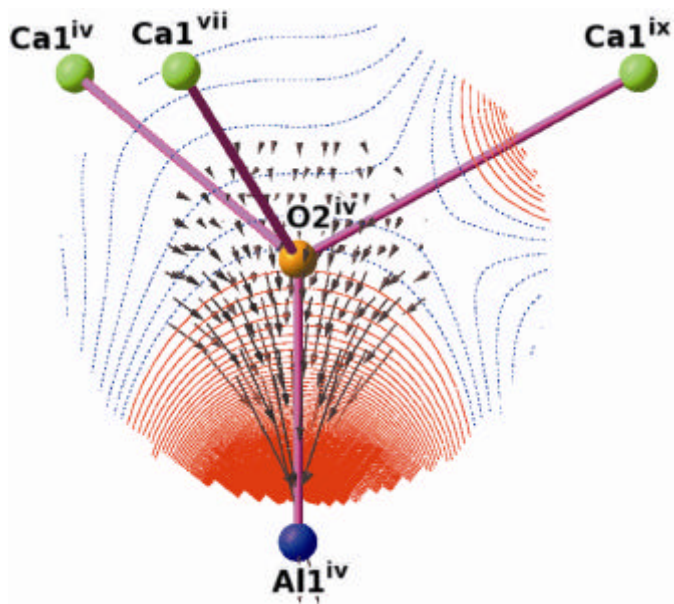


Figure 19 Potential around $O2^{iv}$ on the plane of $Al1^{iv}$, $O2^{iv}$ and $O2a^{iv}$ in the vacant cage. The potential at $O2^{iv}$ is subtracted. Contours are as in Fig.5. $O2a^{vi}$ is behind $O2a^v$.

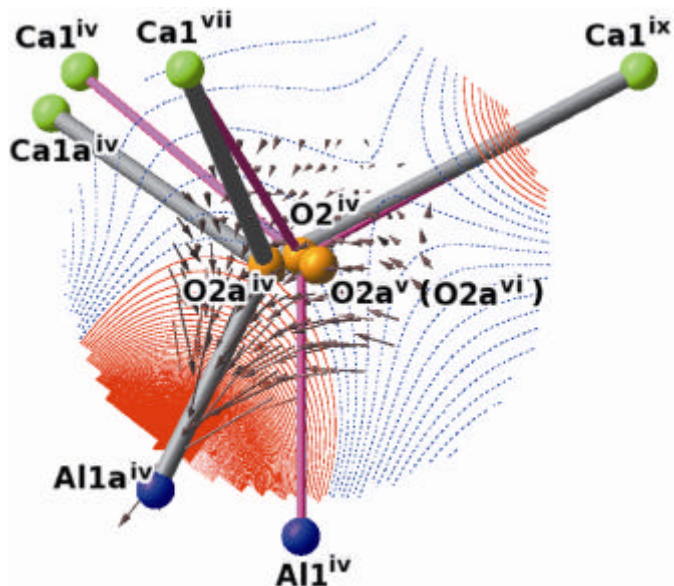


Figure 20 Potential around $O2^{iv}$ on the plane of $Al1^{iv}$, $O2^{iv}$ and $O2a^{iv}$ in the occupied cage. The potential at $O2^{iv}$ is subtracted. Contours are as in Fig.5. $O2a^{vi}$ is behind $O2a^v$.

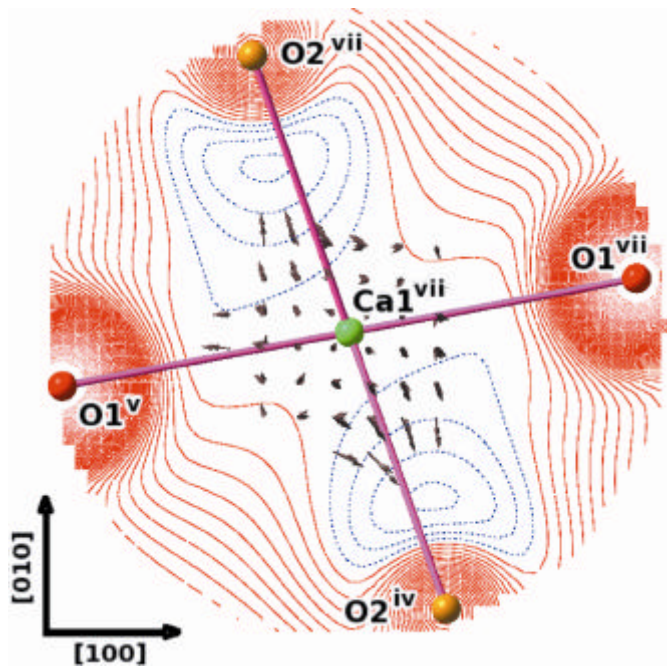


Figure 21 Potential on the plane perpendicular to the two-fold axis including the Ca ion at the centre around Ca1^{vii} in the vacant cage. Potential at Ca ion is normalized to be zero. Contours are as in Fig.5. Ca1c ions are added as dark brown balls.

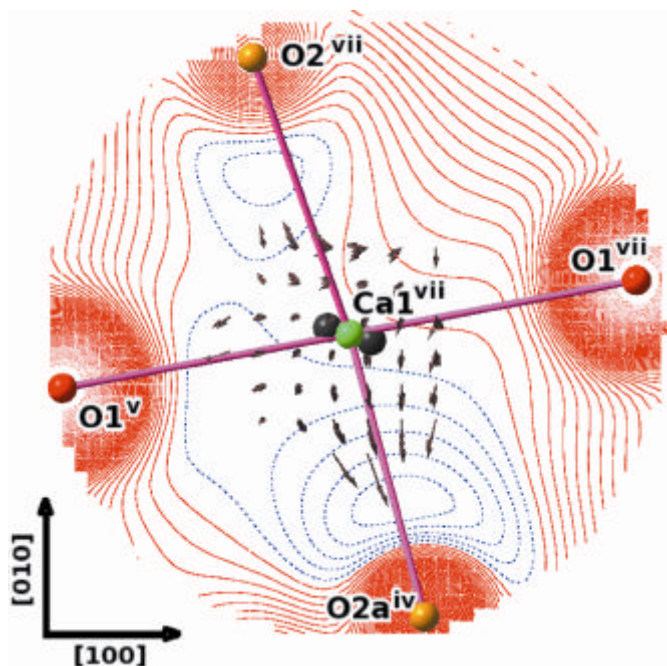


Figure 22 Potential on the plane perpendicular to the two-fold axis including the Ca ion at the centre around Ca1^{vii} in the occupied cage. Potential at Ca ion is normalized to be zero. Contours are as in Fig. 5

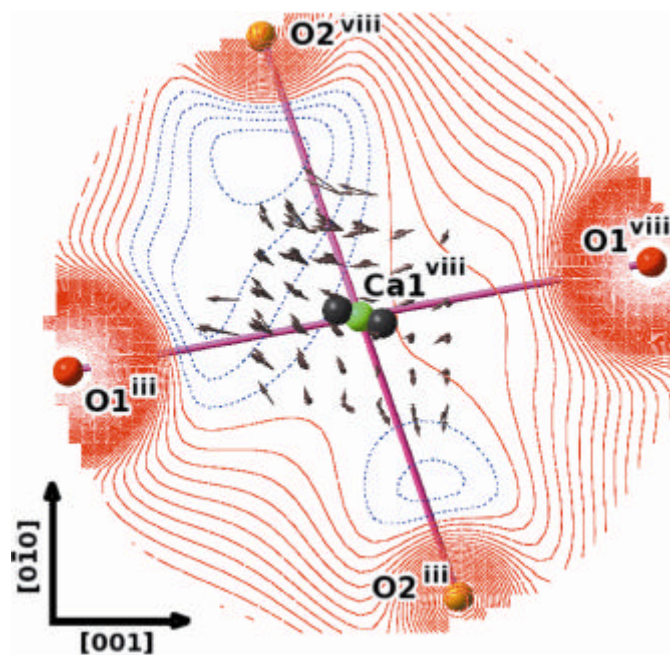


Figure 23 Potential on the plane perpendicular to the two-fold axis including the Ca ion at the centre around Ca1^{viii} in the occupied cage. Potential at Ca ion is normalized to be zero. Contours are as in Fig.5.